Materials Science-Poland, 35(1), 2017, pp. 197-210
http://www.materialsscience.pwr.wroc.pl/
DOI: 10.1515/msp-2017-0017

DE GRUYTER OPEN

The study of structural, elastic, electronic and optical properties of $CsY_x I_{(1-x)}$(Y = F, Cl, Br) using density functional theory

SHABEER AHMAD MIAN[1], MUHAMMAD MUZAMMIL[2], GUL RAHMAN[3,*], EJAZ AHMED[4]

[1]Department of Physics, University of Peshawar, 25120, Peshawar, Pakistan
[2]Computational Nanomaterials Science Lab, Department of Physics Islamia College University Peshawar, Pakistan
[3]Institute of Chemical Sciences, University of Peshawar, 25120, Peshawar, Pakistan
[4]Department of Physics, Abdul Wali Khan University, Mardan, Pakistan

The structural, electronic, elastic and optical properties of $CsY_x I_{(1-x)}$(Y = F, Cl, Br) are investigated using full potential linearized augmented plane wave (FP-LAPW) method within the generalized gradient approximation (GGA). The ground state properties such as lattice constant (a_o) and bulk modulus (K) have been calculated. The mechanical properties including Poisson's ratio (σ), Young's modulus (E), anisotropy factor (A) and shear modulus (G) were also calculated. The results of these calculations are comparable with the reported experimental and theoretical values. The ductility of $CsY_x I_{(1-x)}$ was analyzed using Pugh's rule (B/G ratio) and Cauchy's pressure (C_{12}–C_{44}). Our results revealed that CsF is the most ductile among the $CsY_xI_{(1-x)}$(Y = F, Cl, Br) compounds. The incremental addition of lighter halogens (Y_x) slightly weakens the strength of ionic bond in $CsY_xI_{(1-x)}$. Moreover, the optical transitions were found to be direct for binary and ternary $CsY_xI_{(1-x)}$. We hope that this study will be helpful in designing binary and ternary Cs halides for optoelectronic applications.

Keywords: *alkali halides; structural and electronic properties; DFT; band structure; optical properties*

1. Introduction

In solid-state physics, alkali halide crystals play a prominent role. The wide applications of mixed crystals in optical, electronic and optoelectronic devices evoked considerable interest and motivated researchers to perform extensive investigations [1, 2]. The compounds formed by alkali halides are considered to be a prototype of ionic compounds. The mixed crystals of alkali halides are of disordered substitutional type. They are insulators and crystallize in two types of crystal structures, i.e. body centered cubic and face centered cubic structure [3, 4]. Alkali halides are colored materials when exposed to radiation or impurity doping and thus they are used as detectors due to their strong scintillation effect [5]. Alkali halides are interesting materials in terms of their optical properties and often serve to test new theories [6].

The physical properties of alkali halides (or mixed alkali halides) have been reviewed by Sirdeshmukh et al. [7]. The difference in atomic sizes between mixed crystals causes local stresses in lattice and changes crystal properties, particularly lattice parameter [8, 9]. Recently, several established studies about the absorption spectrum, thermo luminescence, X-ray diffraction, spin-electron resonance, etc., on mixed crystals have been published [10, 11].

The alkali halides usually crystallize in two different phases, i.e. NaCl (B_1) and CsCl (B_2) phase. The space group of NaCl is Fm3m having coordination number of six and containing four atoms per cell, while CsCl belongs to the space group Pm3m having coordination number of eight and two atoms per unit cell. At high temperature, CsCl

*E-mail: gul_rahman47@upesh.edu.pk

structure transforms to NaCl structure, i.e. B_1 phase. At elevated pressure, Rb halides, K halides and NaCl get converted into the CsCI phase [12].

The interest in the high pressure properties of alkali halides has been restored in the diamond cell technology [13]. Cesium halides studies have been carried out to search for the band-overlap metallization which occurs at pressures in the Mbar range. Unexpected phase transformations to tetragonal and orthorhombic structures in the quest of metallization have been observed experimentally and theoretically [14–16].

The absorption spectra of alkali halides contain a large number of peaks which continue to the far ultraviolet region [17]. For example, the emission spectra of heavy metals doped cesium halides are caused by Jahn-Teller effect. The ionic nature (strong or weak) depends on the difference in electronegativity and varies when either of the materials is changed at standard temperature and pressure. Most of the cesium halides crystallize in the BCC form in which both alkali metals and halides have a coordination number of six [18, 19].

Cesium halides CsX (X = F, Cl, Br, I) are inorganic ionic solids and are valuable as radiation detectors or infrared (IR) optical materials in nuclear physics and fuel container technology [20]. Halide structured cesium fluoride (CsF) is used in organic synthesis as a source of fluoride ions [21]. Single crystal of the salt is transparent in deep infrared region and can be used as windows of cells [22].

The chemical bonding and simple morphology of Cs-based halides have made them the preferred choice in several innovative experiments and various theories. Debye's theory of specific heats, Grüneisen's theory of thermal expansion, Born's theory of cohesion, Kellermann's lattice dynamics and Lowdin's very first application of quantum mechanics to crystal elasticity were tested on the alkali halides [23–25].

In this study, we have investigated the structural, elastic, electronic and optical properties of $CsY_x\ I_{(1-x)}$(Y = F, Cl, Br) using GGA and EV-GGA methods. Although the structural and optoelectronic properties of binary alkali halides have been investigated, there are few reports regarding the theoretical study of mixed Cs-based halides. In this study, the calculated values of different parameters such as ductility, band gap, structural and electronic properties of binary and ternary $CsY_xI_{(1-x)}$(Y = F, Cl, Br) have been compared and discussed.

2. Computational method

We have used the FP-LAPW method within the generalized gradient approximation (GGA) [26] and Engel-Vosko generalized gradient approximation (EV-GGA) [27] as implemented in Wien2k code [28] to investigate $CsY_x\ I_{(1-x)}$(Y = F, Cl, Br). Band gaps and electronic dispersion curves are usually underestimated by GGA. In FP-LAPW method, the unit cell is divided into atomic (muffin-tin) spheres and interstitial regions. Inside the muffin-tin sphere, the wave function is expanded in spherical harmonics and the maximum value of l for wave function expansion is taken as $l_{max} = 10$. Plane-waves basis set is used for expansion of wave function, charge density and potential in the interstitial regions. The calculations are performed using a mesh of 1000 k-points in the Brillouin zone (BZ).

3. Results and discussion

3.1. Structural properties

To obtain the structural parameters for all concentrations ($0 \leqslant x \leqslant 1$), optimization of CsY_xI_{1-x} (Y = F, Cl and Br) alloys at the ground state energy was carried out using Birch Murnaghan's equation of state [29]. As an example, the optimized structures of CsBr and $CsBr_{0.25}I_{0.75}$ are given in Fig. 1.

The variation in the unit cell volume optimizes the unit cell energy to the ground state energy of the system as shown in Fig. 2.

Lighter halogens (F, Cl and Br) were doped in CsI. The calculated structural properties such as the lattice constant (a_o), bulk modulus (K), and energy at equilibrium state (E_o) for both B_1 and B_2 phases are shown in Table 1 and Table 2.

Table 1. Structural parameters of CsF_xI_{1-x}, $CsCl_xI_{1-x}$ and $Cs\ Br_xI_{1-x}$ in B_1 phase.

Compound	a [Å]			K [GPa]			E_0
	GGA	Exp.	Other method	GGA	Exp.	Other method	
CsI	7.69	7.52	5.459 [34]	8.72	7 .30 [34]		–29815.72
$CsF_{0.25}I_{0.75}$	7.43			13.91			–105225.63
$CsF_{0.50}\ I_{0.50}$	7.18			11.20			–91188.56
$CsF_{0.75}\ I_{0.25}$	6.76			14.73			–77151.54
CsF	5.99	6.025 [35]	6.12 [36]	35.5			–15778.67
$Cs\ Cl_{0.25}I_{0.75}$	7.44			21.15			–105948.774
$Cs\ Cl_{0.50}I_{0.50}$	7.29			13.77			–92634.72
$Cs\ Cl_{0.75}I_{0.25}$	7.08			15.35			–79320.675
Cs Cl	6.91			20.66			–16501.672
$Cs\ Br_{0.25}I_{0.75}$	7.46			20.25			–110238.56
$Cs\ Br_{0.50}I_{0.50}$	7.36			21.23			–101214.29
$Cs\ Br_{0.75}I_{0.25}$	7.27			11.72			–92190.02
CsBr	7.25		7.23 [32]	9.83		10.45 [34]	–20791.45

Table 2. Structural parameters of CsF_xI_{1-x}, $CsCl_xI_{1-x}$ and $CsBr_xI_{1-x}$ in B_2 phase.

Compound	a [Å]			K [GPa]			E_0
	GGA	Exp.	Other method	GGA	Exp.	Other method	
CsI	4.51	4.57 [37] 4.51 [39]	4.64 [38] 4.52 [36]	10.19	11.9 [37]	12.21 [38] 9.02 [34]	–29815.72
$CsF_{0.25}I_{0.75}$	4.37			14.19			–105225.61
$CsF_{0.50}\ I_{0.50}$	4.21			12.33			–45594.27
$CsF_{0.75}\ I_{0.25}$	3.98			20.48			–77151.50
CsF	3.59	3 [40]	2.99 [34]	35.57		59.17 [34]	–15778.65
$Cs\ Cl_{0.25}I_{0.75}$	4.39			20.52			–105948.78
$Cs\ Cl_{0.50}I_{0.50}$	4.30			16.97			–46317.36
$Cs\ Cl_{0.75}I_{0.25}$	4.18			15.66			–79320.67
Cs Cl	4.08	4.091 [41]	4.11 [36] 3.934 [34]	17.95	22.9 [42]	12.58 [34]	–16501.67
$Cs\ Br_{0.25}I_{0.75}$	4.41			20.03			–110238.57
$Cs\ Br_{0.50}I_{0.50}$	4.39			17.59			–50607.144
$Cs\ Br_{0.75}I_{0.25}$	4.29			15.43			–92190.02
CsBr	4.26	4.23 [39] 4.28 [43]	4.27 [36] 4.069 [34]	15.45	15.6 [39] 17.9 [43]	16.5 [36] 13.01 [34]	–20791.45

As can be seen, the lattice constant exhibits inverse relationship with the dopant concentration. The bulk modulus (K) shows a random variation with increasing doping concentration (x) of halogens. However, for each doping element, the bulk modulus is smaller at $x = 0$ and greater at $x = 1$. In addition, the lattice constant (a_0) and bulk modulus (K) of the materials are in fair agreement with experimental data. Variations of the lattice constant (a_0) and bulk modulus (K) are also plotted vs. concentration (x). Bulk modulus (K) is proportional to crystal rigidity i.e. the larger its value the more rigid is the crystal.

3.2. Elastic properties

Elastic properties of a material can better explain the behavior of a solid under an applied stress. The stability of a material and its stiffness purely depend on elastic properties. These

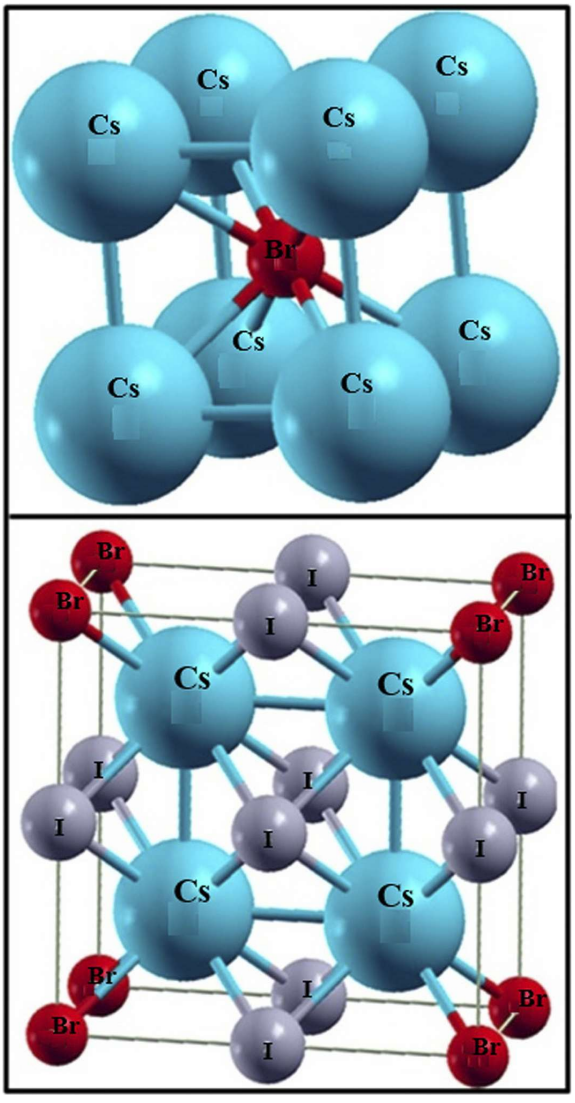

Fig. 1. Top panel: unit cell of binary CsBr (B_2) and bottom panel: unit cell of ternary $CsBr_{0.25}I_{0.75}$.

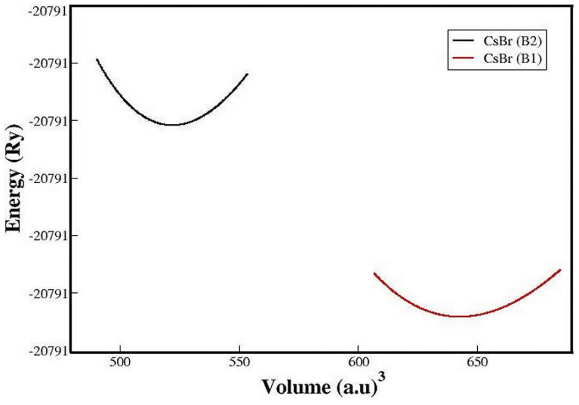

Fig. 2. Energy and volume of B_1 CsF_xI_{1-x} ($0 \leqslant x \leqslant 1$) phase, optimized using GGA method.

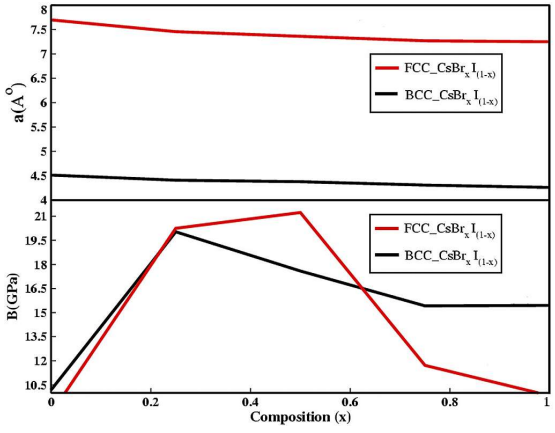

Fig. 3. Plot of bulk modulus and lattice constant of $CsBr_xI_{1-x}$ versus composition.

fundamental properties of a solid can be calculated provided we have stress tensor parameters. Knowing the elastic constants, one can calculate bulk modulus K, Young's modulus E, Poisson's ratio σ, shear modulus G, anisotropy factor A and other physical properties. To describe mechanical properties of cubic compounds CsY (Y = F, Cl, Br and I) we only need to calculate three elastic constants C_{11}, C_{12} and C_{44}.

The elastic and structural parameters of alkali halides are listed in Table 3. It can be seen that the materials show a mix behavior of properties of cubic compounds in both phases. Binary compounds of Cs halides exist in CsCl structure except CsF which exists in NaCl structure at normal conditions. The available experimental and theoretical data concern only the normal phases, in general. We have also calculated the elastic properties of the compounds in other phases i.e. CsCl, CsBr and CsI in FCC structural phase and CsF in BCC phase. Elastically stable cubic structures must satisfy the following relations [30]:

$$(C_{11}/3+2/3C_{12}) > 0(C_{11}-C_{12})/2 > 0 \quad \text{and } C_{44} > 0;\ C_{12} < K < C_{11} \tag{1}$$

The data presented in the Table do not show isotropic behavior which means that

Table 3. The Elastic constants and mechanical properties of alkali halides.

Compound	C_{11}	C_{12}	C_{44}	K	G	E	σ	A	K/G	C_{12}–C_{44}
$CsF(B_1)$	49.43	10.91	23.75	23.752	21.84	50.149	0.15	1.23	1.09	–12.8
CsCl	27.34	7.36	8.967	14.021	9.36	22.977	0.23	0.89	1.50	–1.60
$CsBr(B_1)$	27.05	1.959	4.098	10.321	1.23	3.547	0.44	0.33	8.40	–2.14
CsI	29.19	–1.94	4.887	8.438	7.95	18.142	0.14	0.31	1.06	–6.82
$CsF(B_2)$	55.53	17.47	8.197	30.158	11.57	30.780	0.33	0.43	2.61	9.27
CsCl)	42.33 42.6[c]	–0.02 1.3[c]	3.952 10.9[c]	14.099	8.35	20.920	0.25	0.19	1.69	–3.97
CsBr	28.32 30.97[a] 30[b]	7.36 9.03[a] 7.8[b]	12.95 7.5[a] 7.56[b]	14.348	11.90	27.965	0.18	1.24	1.21	–5.59
CsI	33.98 24.34[a] 24.6[b]	–1.21 6.36[a] 6.7[b]	6.89 6.32[a] 6.24[b]	10.523	10.14	23.030	0.14	0.39	1.04	–8.10

[a][43], [b][44], [c][45]: (a, b, c) experimental values.

the structures are anisotropic [48]. Following equations are used to compute the elastic properties E, G, A, K and σ, etc.:

$$K = \frac{C_{11} + 2C_{12}}{3} \tag{2}$$

$$E = \frac{9GK}{3K + G} \tag{3}$$

$$\sigma = \frac{3K - 2G}{2(3K + G)} \tag{4}$$

$$A = \frac{2C_{44}}{C_{11} - C_{12}} \tag{5}$$

Young's modulus (E) tells us about the stiffness of materials. The greater the value of (E), the stiffer is the material. From Table 3, it is evident that CsF in B_1 phase is stiffer (E = 50.149) as compared to other compounds in both phases. Using elastic constants C_{ij}, Cauchy's pressure C_{12}–C_{44}, the ratio (K/G) Pugh's index of ductility and Poisson's ratio σ we obtain a good prediction of stiffness and ductility. The negative value of Cauchy's pressure represents brittleness, while the positive means that the material is ductile [31]. From Table 3, only CsF in B_2 phase has positive Cauchy's value, while it is negative for all other compounds. Similarly, the higher the ratio K/G, the more ductile is the material and vice versa. The critical value that separates ductility from brittleness is 1.75 [30]. CsF in B_2 phase and CsBr in B_1 phase have this ratio greater than the critical value while for other compounds it is smaller. Poisson's ratio σ is another method to calculate brittleness and ductility of a compound. For a compound to be ductile, the value of its Poisson's ratio must be greater than 0.26, while the one smaller than this value represents the brittle nature [48]. The CsBr in B_1 phase, and CsF in B_2 phase have σ value larger than 0.26 which shows their ductile nature.

3.3. Electronic properties

The energies difference between valence and conduction band determines the electronic properties of materials. Band structures of all binary and their ternary alloys, calculated using two different methods for the compounds in our study; Wu-Cohen GGA and Engel-Vasco (EV) GGA using 1000 k-points grid during DFT simulation, are presented in Fig. 4 to Fig. 7.

Fig. 4 and Fig. 5 represent the energy band structures of binary CsBr in B_1 and B_2 phases, while that of ternary alloy $CsBr_{0.25}I_{0.75}$ are shown in Fig. 6 and Fig. 7.

The calculated band gap values for binary compounds and their ternary alloys in B_1 phase are tabulated in Table 4, while for B_2 phase are presented in Table 5 along with experimental and other theoretically calculated values. Most of the band structures of the binary and ternary alloys are direct band gap. The results obtained using Wu-Cohen GGA and EV-GGA for binary compounds reveal that the band gap (E_g) is smaller for rock salt phase

Table 4. Energy band gaps for F, Cl and Br doped CsI in rock salt (B_1) phase for ($0 \leqslant x \leqslant 1$).

B_1	GGA E_g [eV]	EV-GGA E_g [eV]	Experimental E_g [eV]
CsI	3.7026	3.678	
$CsF_{0.25}I_{0.75}$	3.6043	4.3164	
$CsF_{0.50}I_{0.50}$	3.9481	4.4391	
$CsF_{0.75}I_{0.25}$	4.3163	4.7583	
CsF	5.3966	6.3786	9.8 [45]
$CsCl_{0.25}I_{0.75}$	4.1690	4.9792	
$CsCl_{0.50}I_{0.50}$	4.3163	5.0529	
$CsCl_{0.75}I_{0.25}$	4.3900	5.151	
CsCl	4.8319	5.814	
$CsBr_{0.25}I_{0.75}$	4.0954	4.9792	
$CsBr_{0.50}I_{0.50}$	4.1199	5.0283	
$CsBr_{0.75}I_{0.25}$	4.2181	4.9547	
CsBr	4.0463	5.1265	

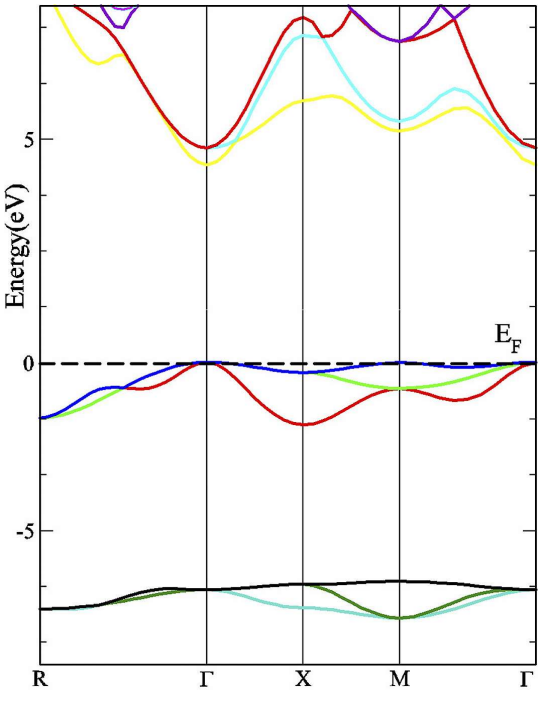

Fig. 4. Band structure of binary Cs halides (CsBr) obtained with Wu-Cohen GGA.

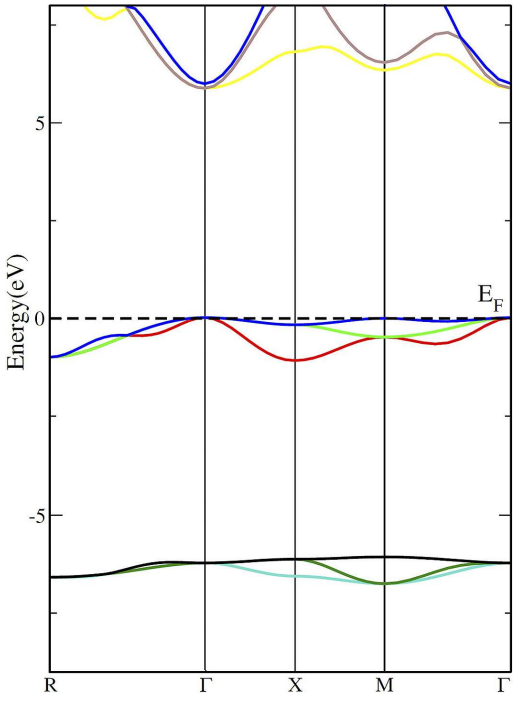

Fig. 5. Band structure of binary Cs halides (CsBr) obtained with EV- GGA.

of cesium halides than B_2 phase, while for CsCl band gap in B_1 phase is larger than B_2 only in EV-GGA scheme. Similarly, the band gap calculated for binary cesium halides using Wu-Cohen GGA is smaller than EV-GGA except for CsI (B_1 phase). Band gap is larger as EV-GGA method has been used for B_2 phase. This increase is also observed in the case of all ternary alloys in both

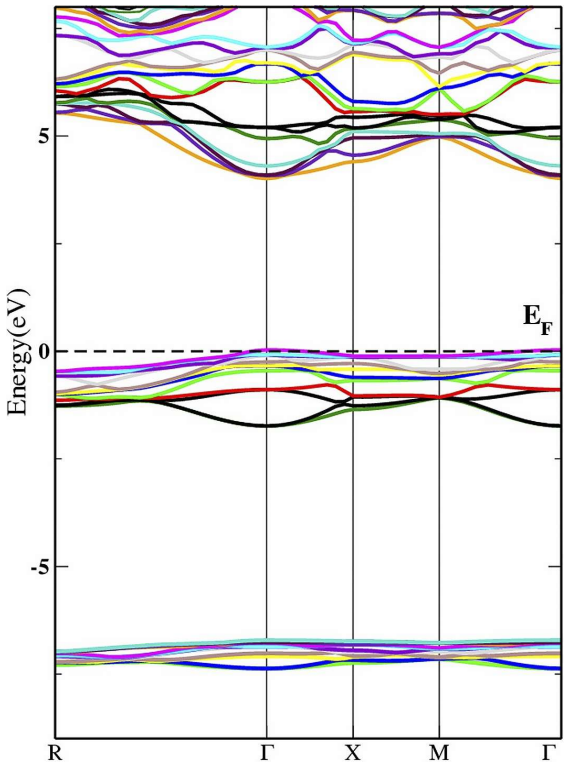

Fig. 6. Band structure of Br doped CsI at x = 0.25 in FCC phase obtained by Wu-Cohen GGA.

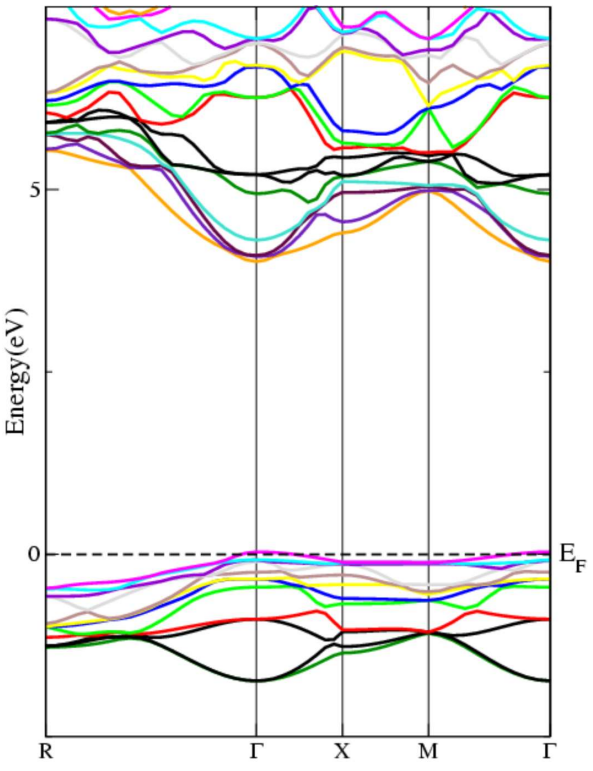

Fig. 7. Band structure of Br doped CsI at x = 0.25 in FCC phase obtained by EV- GGA.

phases calculated using EV-GGA method. Furthermore, the increase in band gap is proportional to the dopant concentration in all cases and phases.

3.4. Density of states

Density of states (DOS) is an important tool to determine different electronic states, dielectric function, reflectivity and band structure of solids.

In Fig. 8, total and partial density of states are given at all concentrations ($0 \leqslant x \leqslant 1$) and in both phases of $CsY_x\ I_{(1-x)}$(Y = F, Cl, Br) using Wu-Cohen GGA scheme. In the figure of binary compounds and ternary alloys of B_1 and B_2 phases, mixed d-states of all the elements contribute in a very small proportion in conduction band, whereas far region of conduction band is upheld by Cs f-state with a very minute contribution. Fluorine p-state gives a separate peak in all compounds and in both phases (binary as well as ternary) in the valence band near Fermi level. The second sharp peak in the valence band region of CsCl and CsBr corresponds to the halogen p-state, excluding fluorine. The third peak at the lower energy side of valence band is purely the contribution of Cs p-state. In the density of states plot, overall behavior of all compounds is the same for both phases shown in Fig. 8. This behavior is attributed to the overlapping of energy states to form a ternary alloy.

3.5. Electron density

To assess the probability of identifying the specific location of electrons and to obtain information about the nature of bonds among the atoms of a molecule, electron density calculations are important. In the present work, the electron density has been calculated in CsY_xI_{1-x}(Y = Br, F and Cl) in rock salt phase as well as CsCl structure using the generalized gradient approximation (GGA) method. The bonding nature is ionic in which charge transfer between the anion and cation occurs.

Table 5. Energy band gaps for F, Cl and Br doped CsI in B_2 phase for ($0 \leqslant x \leqslant 1$).

B_2	GGA E_g [eV]	EV-GGA E_g [eV]	Experimental E_g [eV]	Other calculations E_g [eV]
CsI	3.8744	5.0283	6.2 [46] 6.50 [32]	3.91 [39] 3.97 [33]
$CsF_{0.25}I_{0.75}$	3.7762	4.611		
$CsF_{0.50}I_{0.50}$	4.1445	4.8319		
$CsF_{0.75}I_{0.25}$	4.3163	5.0529		
CsF	5.9858	7.361		
$CsCl_{0.25}I_{0.75}$	4.0463	4.7828		
$CsCl_{0.50}I_{0.50}$	4.2918	4.9546		
$CsCl_{0.75}I_{0.25}$	4.3654	5.0529		
CsCl	5.2493	5.2247	7.90 [32]	5.27 [33]
$CsBr_{0.25}I_{0.75}$	3.9972	4.8319		
$CsBr_{0.50}I_{0.50}$	4.1199	5.0283		
$CsBr_{0.75}I_{0.25}$	4.1199	5.0774		
CsBr	4.3900	5.8385	7.30 [32]	4.56 [33]

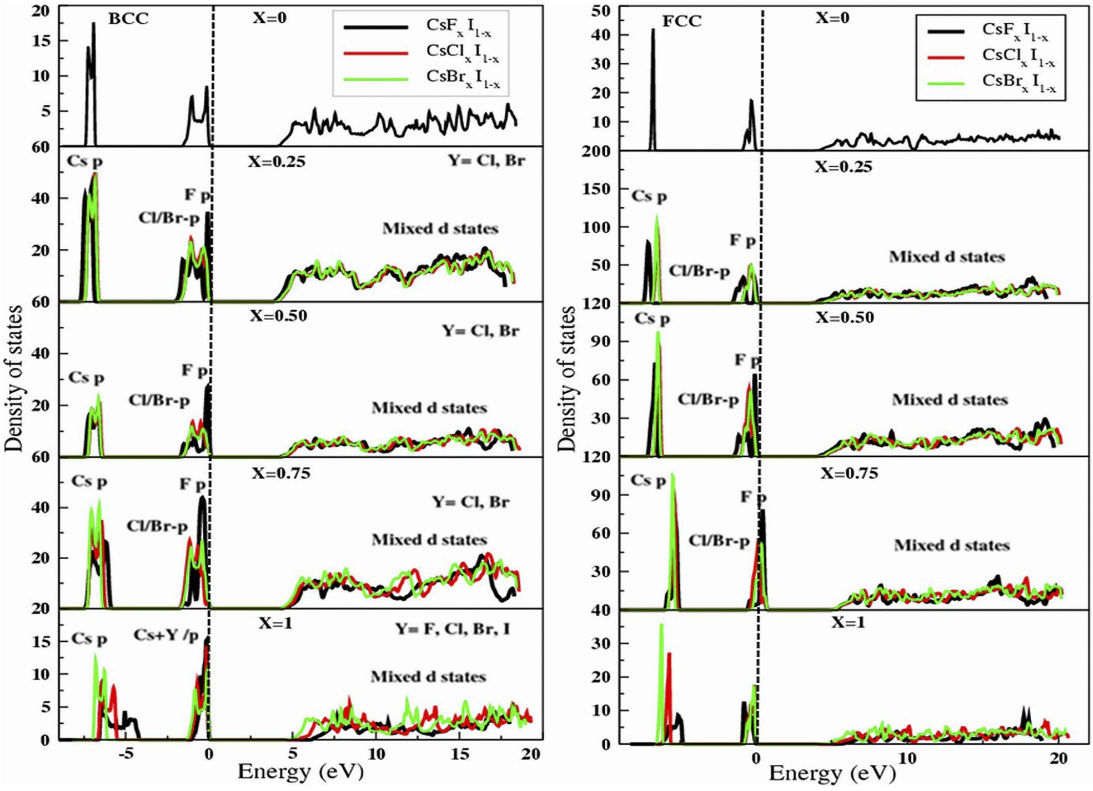

Fig. 8. DOS for CsY_xI_{1-x} at concentrations ($0 \leqslant x \leqslant 1$). Substate p contributes the most in the valence band, while the mixed d-states contribute the most in the conduction band.

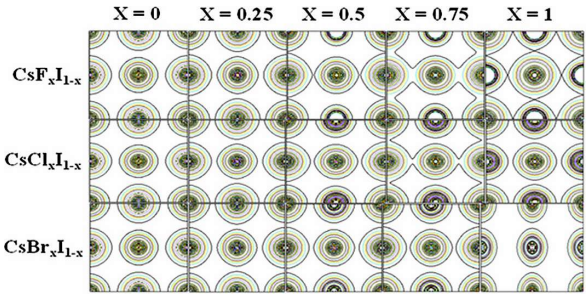

Fig. 9. Contour of electron density for F, Cl and Br doped cesium iodide at ($0 \leqslant x \leqslant 1$) in B_1 phase along (1 1 0) plane.

The electron density plots for CsY_xI_{1-x} at different concentrations are plotted in Fig. 9 in (1 1 0) plane for B_1 phase and Fig. 10 in (0 1 1) plane for B_2 phase.

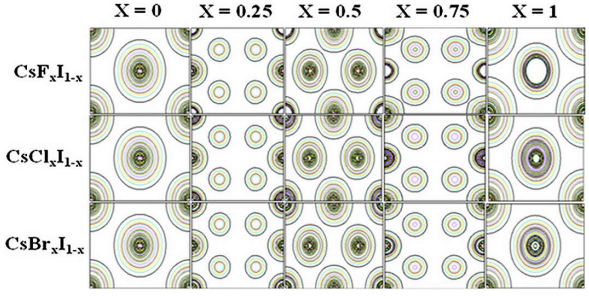

Fig. 10. Electron density of F, Cl and Br doped cesium iodide at ($0 \leqslant x \leqslant 1$) in B_2 phase along (0 1 1) plane.

The first column in both figures represents CsI with increasing concentration (x = 0.25, 0.50, 0.75 and 1) of halogens in the order of F, Cl and Br, respectively. From the plots of these compounds it is revealed that the boding nature is mostly ionic since there is a strong localization of the charge around the anion side. The contour plots are expressed in the units of electrons per unit cell. It is observed that doping of lighter halogens produced slightly covalent character in binary compounds which are pure ionic in nature. In B_1 phase of CsF, the covalent character is strong as compared to other binary Cs halides because fluorine is the smallest halogen atom while the ternary alloys, $CsF_{.75}I_{.25}$ and $CsCl_{.75}I_{.25}$ show the most covalent character out of all in B_1 phase. The rest of all binary compounds and ternary alloys are ionic in both phases.

3.6. Optical properties

The dielectric functions for CsY_xI_{1-x} in the energy range of 0 eV to 40 eV are presented in Fig. 11 and Fig. 12 showing the real $\epsilon_1(\omega)$ and imaginary $\epsilon_2(\omega)$ parts for all concentrations in B_1 and B_2 structure.

In the left panel of Fig. 11 and Fig. 12, $\epsilon_1(\omega)$ is the real part while in the right panel of the figures, imaginary part $\epsilon_2(\omega)$ is shown. The positive value of the real part at low frequency is the static part of the dielectric constant. After reaching the maximum value, the dielectric constant decreases with frequency and some peaks with negative values appear. This corresponds to the metallic region of materials that exhibit negative values of $\epsilon_1(\omega)$. From Fig. 12 it is noted that different peaks appear in the spectra of the compounds and the alloys. The transition of electrons from the occupied states of the valence band to the unoccupied states of the conduction band causes the appearance of the peaks.

In CsF_xI_{1-x} with B_1 phase at x = 0 the real part $\epsilon_1(\omega)$ is positive for all energy ranges but is negative in the energy ranges of 7.52 eV to 8.79 eV and 14.12 eV to 17.47 eV which gives maximum peak 5.31 at energy 4.74 eV. The imaginary part $\epsilon_2(\omega)$ indicates two peaks: the maximum peak 5.30 at energy 7.28 eV and second 4.28 at 5.97 eV. As the concentration of lighter halogens was increased, the maximum peak decreases in both real and imaginary parts of dielectric function. This reflects that the behavior of the material has shifted from lower to higher energy values as the dopant concentration is increased. This is observed in both real and imaginary parts of dielectric function. Reflectivity is the ratio of the reflected power to the incident power of the material. The reflectivity (R) is plotted for CsY_xI_{1-x} for concentrations x ($0 \leqslant x \leqslant 1$) as shown in the Fig. 13.

Binary CsI (B_1) reflectivity is maximum in energy range from 5 eV to 10 eV (0.29) and from 15 eV to 20 eV (0.38) and it decreases at high energy. Fluorine doped CsI peak diminishes with increasing concentration x = from 0 to 1. Furthermore, no significant peak changes are observed in the range of 15 eV to 20 eV. By chlorine doping

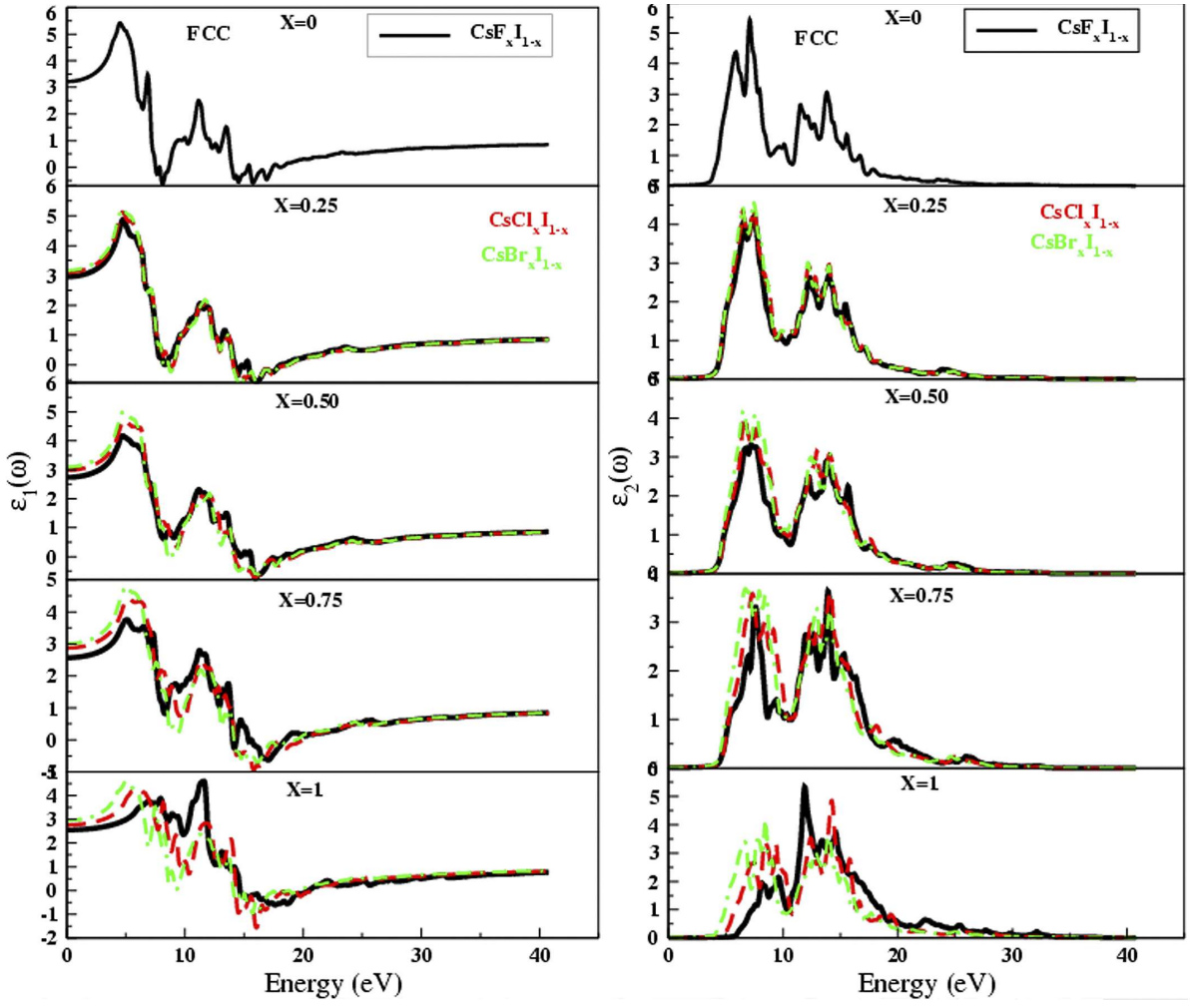

Fig. 11. Real and imaginary parts of dielectric function for CsY_xI_{1-x} (Y = F, Cl and Br) for the concentration x ($0 \leqslant x \leqslant 1$) in B_1 phase.

into CsI, the peak reduces in a similar way with increasing concentration while slight increase is observed in the range of 15 eV to 20 eV. The reflectivity at x = 0.25, 0.50, 0.75 and 1 is given as 0.33, 0.34, 0.37 and 0.47, respectively. Slight peaks change from 0.28 to 0.23 is observed in bromine doping in the range of 5 eV to 10 eV. The observed changes are very clear in the second set of peaks from 0.29 to 0.37 with bromine doping for x equal to 0, 0.25, 0.5, 0.75, and 1.0.

In B_2 structure of CsI, maximum reflectivity (0.38) is found in the energy range from 5 eV to 10 eV and the second set of two peaks with reflectivity of 0.35 is located in 15 eV to 20 eV energy range. Fluorine doping with x = 0.25, 0.50, 0.75 and 1 in the range of 15 eV to 20 eV changes the peaks to 0.39, 0.41, 0.45 and 0.48, respectively, whereas the peak in the range of 5 eV to 10 eV decreases from 0.37 to 0.17. For chlorine doping, two peaks in the energy range 5 eV to 10 eV are evident which shift from 0.28 and 0.30 at x = 0.25 to 0.24 and 0.25 at x = 1 (CsCl). Two more intense peaks in the energy range of 15 eV to 20 eV change from 0.39 and 0.35 at x = 0.25 to 0.49 and 0.39 at x = 1. These clearly indicate that increasing dopant concentration results in larger peaks but at higher photon energies. Finally, in case of bromine, two peaks in the range of 5 eV to 10 eV decrease with increasing dopant concentration from 0.29 and 0.32 at x = 0.25 to 0.25 and 0.29 at x = 1. The peaks

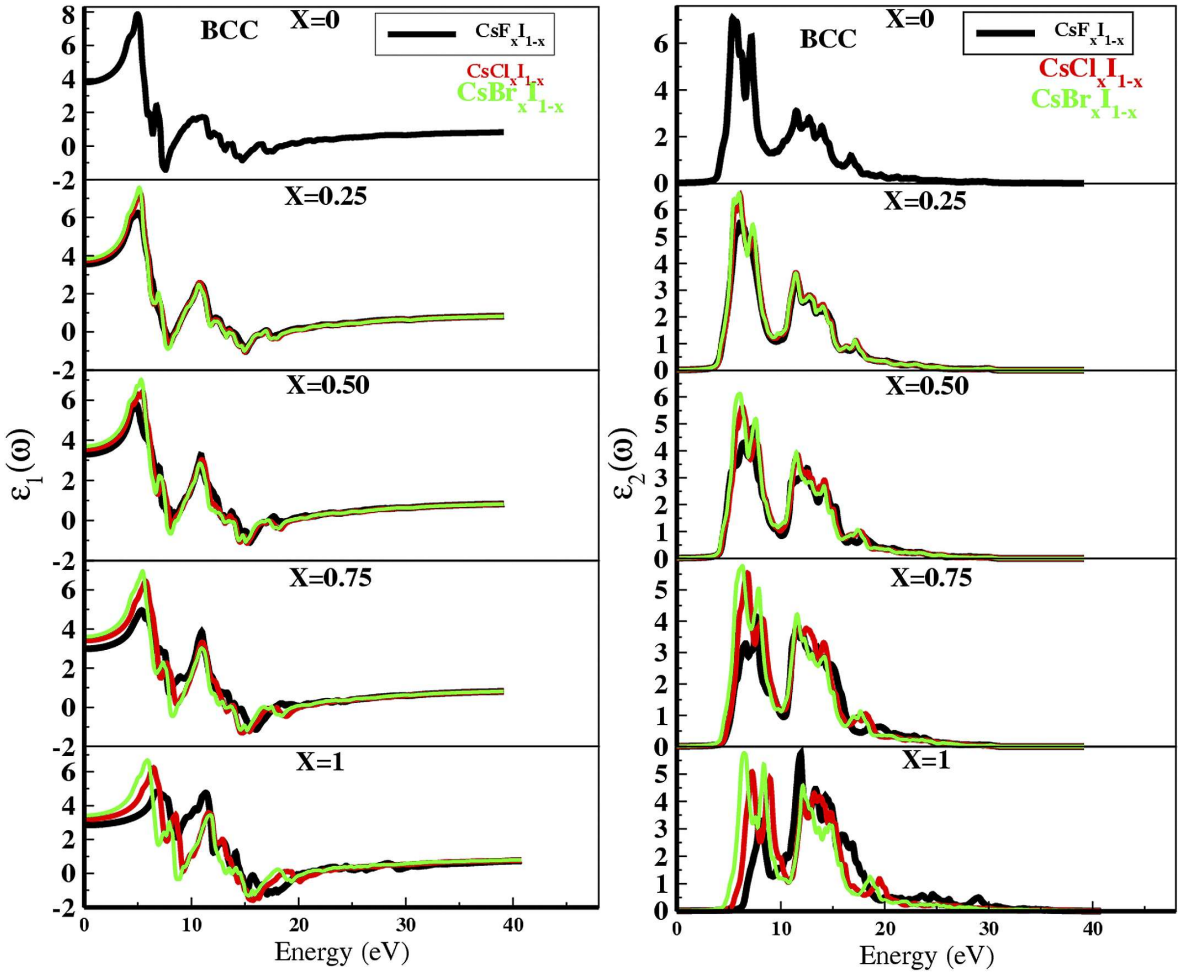

Fig. 12. Real and imaginary parts of dielectric function for CsY_xI_{1-x} (Y = F, Cl and Br) for the concentration x ($0 \leqslant x \leqslant 1$) in B_2 phase.

observed in the range of 15 eV to 20 eV increase from 0.39 and 0.36 at x = 0.25 to 0.44 and 0.39 at x = 1.

3.7. Optical conductivity

The electron transportation in a material can be observed by optical conductivity (σ). In Fig. 14, optical conductivity of CsY_xI_{1-x} at different concentrations for both B_1 and B_2 structures is presented.

The conductivity changes in the range of 4 eV to 40 eV for all compounds with different concentrations. It is observed that for BCC phase optical conductivity shifts to higher energy with increasing concentration, whereas in FCC structure, one of the two peaks gets smaller.

In binary CsI (B_1), two peaks of 5080 $\Omega^{-1}\cdot cm^{-1}$ and 5577 $\Omega^{-1}\cdot cm^{-1}$ are located, respectively, at 7.26 eV and 13.89 eV. Finally, the conductivity decreases and approaches to zero at 39 eV. The decreasing behavior in the peak values of optical conductivity is observed when the halogens are doped at concentrations x = 0.25, 0.5, 0.75 and 1.

The optical conductivity for B_2 phase of CsY_xI_{1-x} is also shown Fig. 14. The highest peak is found for pure CsI (6222 $\Omega^{-1}\cdot cm^{-1}$) at 7.7 eV, while there is a set of three peaks (4860 $\Omega^{-1}\cdot cm^{-1}$) lying in energy range of 12 eV to 14.5 eV. By fluorine doping in B_2 phase CsI, the first peak shifts from 6222 $\Omega^{-1}\cdot cm^{-1}$ to 3459 $\Omega^{-1}\cdot cm^{-1}$, when

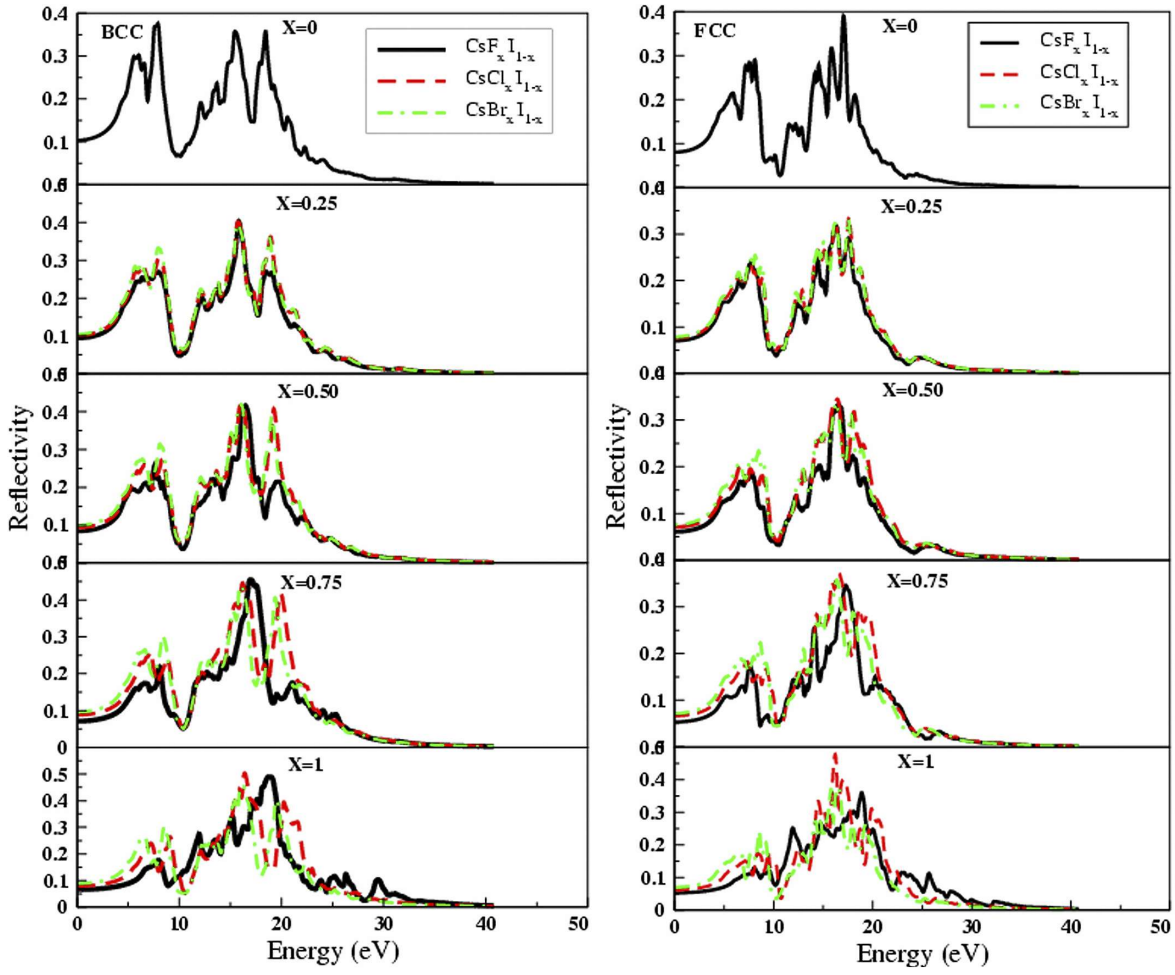

Fig. 13. Reflectivity vs. energy (eV) plot for Y (Y = F, Cl and Br) doped CsI in B_1 and B_2 phases. At very low and high energy values, R is less than 10 % which means that the material is transparent. Effect of doping with lighter halogens is the increase in reflectivity which is the highest at x = 1.

the concentration varies from x = 0 to 1, while the second peak increases as concentration increases, i.e. from 4860 $\Omega^{-1}\cdot cm^{-1}$ to 9099 $\Omega^{-1}\cdot cm^{-1}$ at x changing from 0 to 1. Introduction of chlorine (Cl) caused that the plot of optical conductivity shows three major peaks, two in the energy range of 6 eV to 10 eV, while the third one lies between 12 eV and 14 eV. The very first peak keeps decreasing with increasing Cl content, while the second one decreases till x = 0.75 and then starts to increase for x = 1 (CsCl). The third peak increases with Cl concentration and has the highest value of 7803 $\Omega^{-1}\cdot cm^{-1}$ at x = 1 (CsCl) at energy of 13.6 eV. After addition of bromine (Br), CsI shows three major peaks. Two of them are in the energy range of 6 eV to 9 eV, while the third one is in the range of 11.5 eV to 12.5 eV. The first peak decreases with an increase in Br concentration. The second peak is of the same height as that of the first one but it gradually increases from 5521 $\Omega^{-1}\cdot cm^{-1}$ to 5821 $\Omega^{-1}\cdot cm^{-1}$ (CsBr). The third peak keeps increasing till it attains a maximum value of optical conductivity (7346 $\Omega^{-1}\cdot cm^{-1}$) at 12.2 eV for CsBr (B_2) phase.

4. Conclusions

The GGA, EV-GGA potentials were applied to study the bonding nature and optoelectronic properties of CsY_xI_{1-x} compounds. In cubic phase,

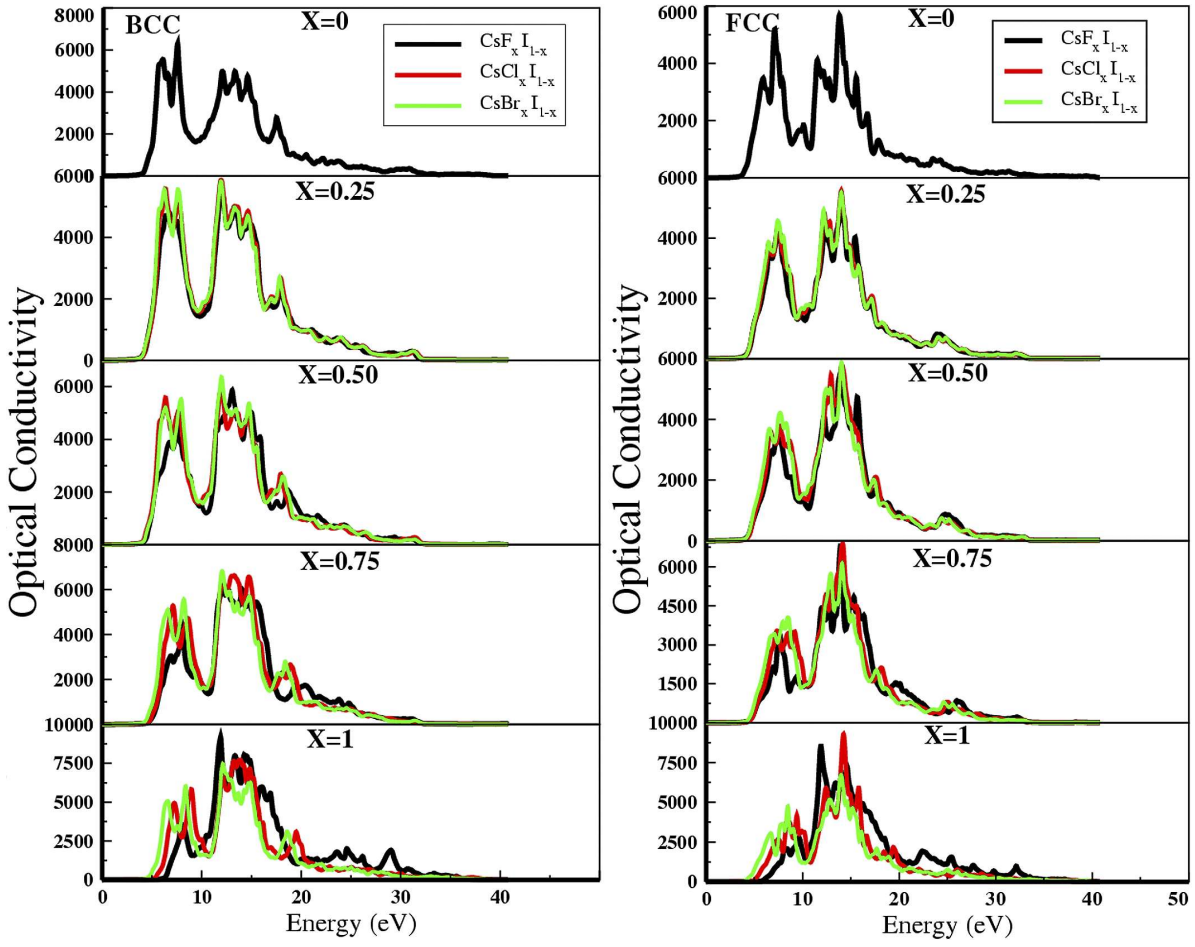

Fig. 14. Optical conductivity vs. energy for Y (Y= F, Cl, and Br) doped CsI at concentration ($0 \leqslant x \leqslant 1$).

the structural properties and density of states (DOS) have been calculated for further theoretical and experimental investigations. It is worth noting that our calculated structural properties for CsY_xI_{1-x} compounds match well with available experimental data, better than other theoretical results. From the structural properties, it has been demonstrated that bulk modulus decreases in both B_1 and B_2 phases and is responsible for low compressibility and high hardness.

The bonding analysis and electron density revealed that most of binary and ternary halides of Cs are ionic except for few showing a minute contribution of covalent bonding. High absorption peaks and reflectivity are observed in the visible and ultraviolet (UV) region of the energy spectrum. CsCl in B_1 phase shows the highest reflectivity among all others. This study can be helpful in designing these materials for devices such as Bragg's reflectors, optical and optoelectronic devices working in UV region of spectrum.

Acknowledgements

The authors acknowledge the support from the Institute of Chemical Sciences, University of Peshawar, Department of Physics University of Peshawar and Islamia College University Peshawar for providing research facilities.

References

[1] DESHMUKH D.B., SRINIVAS K., *J. Mater. Sci.* 21(1986), 4117.
[2] NIKL M., *Phys. Status. Solidi. A*, 178 (2000), 596.
[3] BABU V.H., RAO U.V.S., *Prog. Cryst. Growth. Ch.*, 8 (1984), 189.
[4] CORTONA P., *Phys. Rev. B*, 46 (1992), 2008.
[5] GONÇALVES G.C., LALIC M.V., MALTA O.L., *Acta Phys. Pol. A*, 112 (2007), 1043.

[6] ERWIN S.C., LIN C.C., *J. Phys. C-Solid State Phys.*, 21 (1988) 4285.
[7] SIRDESHMUKH D.B., SRINIVAS K., *J. Mater. Sci.*, 21 (1986), 4117.
[8] SCHULMAN J.H., COMPTON W.D., *Color Centers in Solids*, Pergarmon Press, New York, 1963.
[9] FOWLER W.B., *Physics of Color Centers*, Academic Press, New York, 1968.
[10] PERUMAL S., MAHADEVAN C.K., *Physica B*, 369 (2005), 89.
[11] KUMARI R.A., CHANDRAMANI R., *Radiat. Meas.*, 43 (2008), 278.
[12] PAULING L., *J. Am. Chem. Soc.*, 54 (1954), 3570.
[13] NARDELLI M.B., BARONI S., GIANNOZZI P., *Phys. Rev. B*, 51 (1995), 8060.
[14] SAITTA A.M., ALFČ D., DE GIRONCOLI S., BARONI S., *Phys. Rev. Lett.* 78 (1997), 4958.
[15] LIU J., DUBROVINSKY L., BALLARAN T., CRICHTON W., *High Pressure Res.* 27 (2007), 483.
[16] SMIRNOV N.A., *Phys. Rev. B*, 83 (2011), 014109.
[17] SONG K.S., WILLIAMS R.T., *Self-trapped excitons*, Springer Science & Business Media, Berlin, 2013.
[18] EBY J.E., TEEGARDEN K.J., DUTTON D.B., *Phys. Rev.*, 116 (1959), 1099.
[19] DROTNING W.D., DRICKAMER H.G., *Phys. Rev. B*, 14 (1976), 3706.
[20] WELLS A.F., *Structural Inorganic Chemistry*, Clarendon Press, Oxford, 1984.
[21] PEREIRA M.C.C., FILHO T.M., HAMADA M.M., *Nukleonika*, 54 (2009), 151.
[22] SHARMA V., TIWARI S., AHUJA B.L., *Radiat. Phys.Chem.*, 79 (2010), 678.
[23] GREENWOOD N.N., EARNSHAW A., *Chemistry of Elements*, Pergamon Press, Oxford, 1984.
[24] SIRDESHMUKH D.B., SIRDESHMUKH L., SUBHADRA, K.G., *Alkali halides: A Handbook of Physical Properties*, Springer, Berlin, 2001.
[25] SCHWARZ K., *J. Solid State Chem.*, 176 (2003), 319.
[26] MAYER J.E., *J. Chem. Phys.*, 1 (1933), 270.
[27] STUART B., *Infrared spectroscopy*, in: *Kirk-Othmer Encyclopedia of Chemical Technology*, Wiley, New York, 2005.
[28] ZHIGANG W., COHEN R.E., *Phys. Rev. B*, 73 (2006), 235116.
[29] ENGEL E., VOSKO S.H., *Phys. Rev. B*, 50 (1994), 10498.
[30] SCHWARZ K., BLAHA P., MADSEN G.K.H., *Comput. Phys. Commun.*, 147 (2002), 71.
[31] PETTIFOR D.G., *Mater. Sci. Tech-Lond.*, 8 (1992), 345.
[32] VAITHEESWARAN G., KANCHANA V., KUMAR R.S., CORNELIUS A.L., NICOL M.F., SVANE A., DELIN A., JOHANSSON B., *Phys. Rev. B*, 76 (2007), 014107.
[33] TOHYAMA T., MAEKAWA S., *J. Phys. Soc. Jpn.*, 60 (1991), 53.
[34] SMITH J.A., PONG W., *Phys. Rev. B*, 12 (1975), 5931.
[35] KIGUCHI M., ENTANI S., SAIKI K., KOMA A., *Surf. Sci.*, 523 (2003), 73.
[36] PENDAS A.M., RECIO J.M., FRANCISCO E., LUANA V., *Phys. Rev. B*, 56 (1997), 3010.
[37] OHTAKI H., FUKUSHIMA N., *Pure Appl. Chem.*, 63 (1991), 1743.
[38] CORTONA P., *Phys. Rev. B*, 46 (1992), 2008.
[39] SATPATHY S., *Phys. Rev. B*, 33 (1986), 8706.
[40] RIBEIRO R.M., COUTINHO J., TORRES V.J.B., JONES R., SQUE S.J., OBERG S., SHAW M.J., BRIDDON P.R., *Phys. Rev. B*, 74 (2006), 035430.
[41] VALLIN J., BECKMAN O., SALAMA K., *J. Appl. Phys.*, 35 (1964), 1222.
[42] IVEY H.F., *Phys. Rev.*, 72 (1947), 341.
[43] GANESAN V., GIRIRAJAN K.S., *Pramana-J. Phys.*, 27 (1986), 469.
[44] SINGH R.K., GUPTA H.N., AGRAWAL M.K., *Phys. Rev. B*, 17 (1978), 894.
[45] REINITZ K., *Phys. Rev.*, 123 (1961), 1615.
[46] SPANGENBERG K., HAUSSUHL S., *Z. Kristallogr.*, 109 (1957), 422.
[47] SLAGLE O.D., MCKINSTRY H.A., *J. Appl. Phys.*, 38 (1967), 451.
[48] TEEGARDEN K., BALDINI G., *Phys. Rev.*, 155 (1967), 896.

Received 2016-05-16
Accepted 2016-12-19